SUPPLEMENTARY FIGURES

Hsu et al.

SUPPLEMENTARY FIGURE LEGEND

Supp. Fig. 1. K. lactis est1Δ mutant exhibit senescence and telomere shortening.

(A) The *K. lactis est1Δ* strain was passaged on YPD medium. Colonies that have undergone the indicated number of generations were re-streaked together on two plates. Some small colonies suggestive of senescence can be observed at 75 and 100 generations (black arrowheads). More severe and uniform growth defects are seen at 175 and 200 generations.

(B) An *est1Δ* clone and one bearing wild type *EST1* on a plasmid were passaged and their telomeres analyzed after the indicated number of streaks.

Fig. S2. Growth defects of K. lactis EST1 mutants

The *K. lactis est1Δ* mutant reconstituted with the indicated *EST1* alleles were passaged on YPD medium. Colonies that have undergone the indicated number of generations were re-streaked together.

Fig. S3. Characterization of the KlEst1 K467E mutant.

(A) The expression of *Kl*Est1$_{NTD}$-TAP and *Kl*Est1$_{NTD\text{-}K467E}$-TAP (marked by an arrow) in the reconstituted strains was analyzed by IgG-Sepharose pull down and Western using anti-protein A antibodies.

(B) The binding of *Kl*Est1$_{NTD}$-TAP and *Kl*Est1$_{NTD\text{-}K467E}$-TAP to Ter1 in cell extracts was analyzed by IgG-Sepharose pull down and RT-PCR. The levels of U1 in the pull down samples were also measured and used as controls for non-specific binding.

(C) The *est1* null mutant was transformed with plasmids that contain either *Kl*Est1-TAP or *Kl*Est1$_{K467E}$-TAP. The resulting strains were passaged in selective media and their telomeres analyzed by Southern after 1, 3 and 5 streaks.

Fig. S4. KlEst1 interacts with RNA in an RNA concentration- and sequence-dependent manner.

(A) Purified Est1 (12.5 nM) was incubated with increasing concentrations of ^{32}P-labeled Ter1$_{EBD}$, antisense Ter1$_{EBD}$, and CS2a-sub (1, 2, 4, 8, 16 nM), and subjected to the RNA-protein UV crosslinking assay. The products were analyzed by SDS-PAGE and visualized by a PhosphorImager. (B) The relative crosslinking signals from (A) were quantified and plotted.

Fig. S5. The KlEst1 residues required for RNA-binding.

A homology model of *Kl*Est1$_{NTD}$ was generated using the I-TASSER server and displayed in surface representations. The TPR subdomain, the DSH subdomain, and the mutation clusters are colored in yellow, green, and red, respectively. The putative peptide-binding groove is labeled "P". The bottom view is related to the top view by a 90° rotation in the x-axis.

Fig. S6. A conserved basic residue in Est1 is required for telomerase RNA-binding in budding and fission yeast.

An alignment of the TPR domain of selected budding and fission yeast Est1 homologues is displayed. Budding yeast and *S. pombe* Est1residues implicated in RNA-binding are

indicated by filled and open circles, respectively. The locations of α helices within the TPR domain are designated by cylinders below the alignment.

Supp. Fig. 1

A

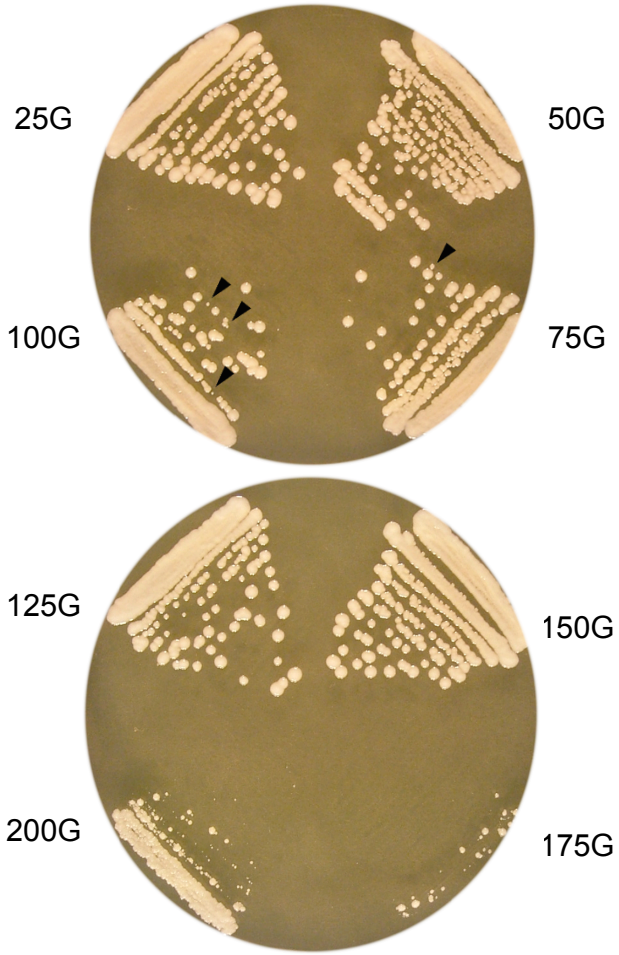
25G
50G
100G
75G
125G
150G
200G
175G

B

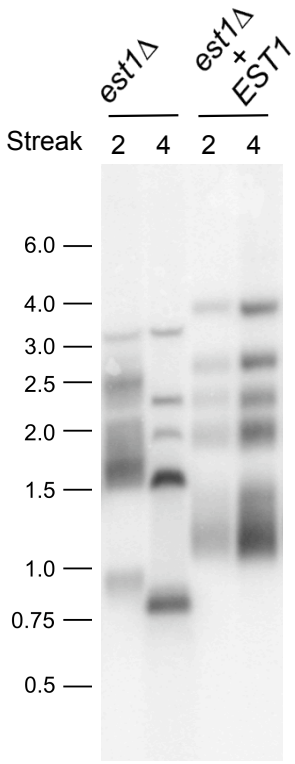
est1Δ
est1Δ + EST1
Streak
2
4
2
4
6.0
4.0
3.0
2.5
2.0
1.5
1.0
0.75
0.5

Supp. Fig. 2

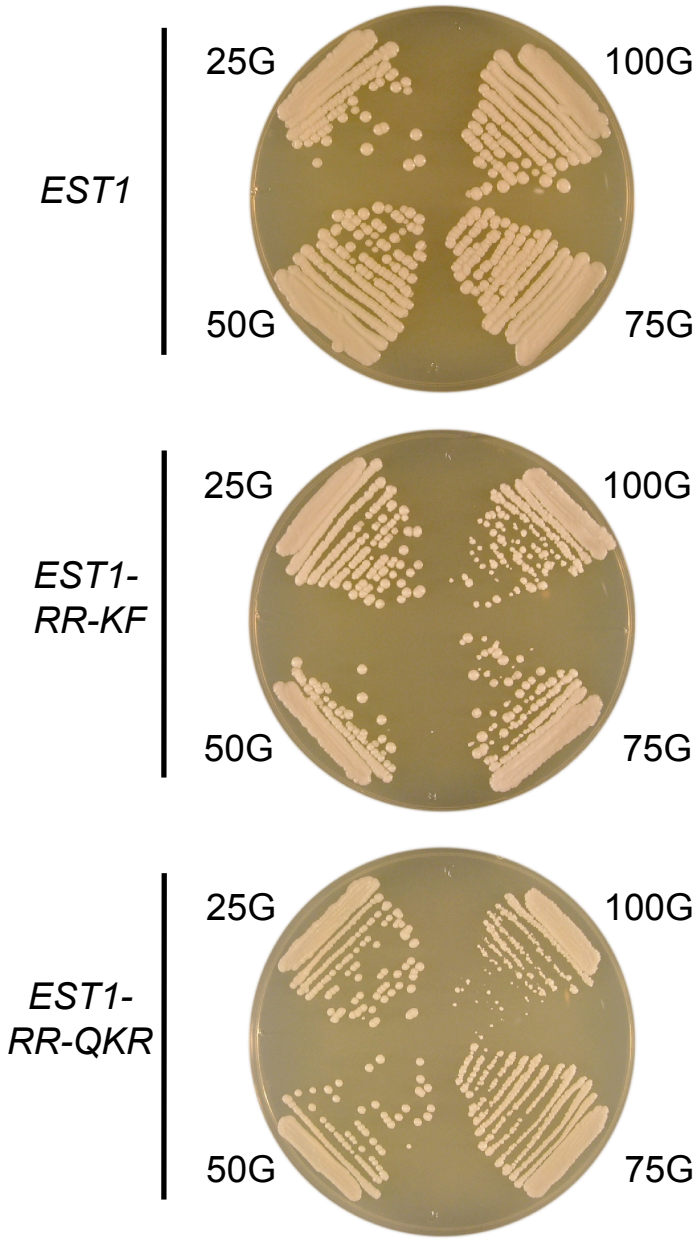
EST1
25G
100G
50G
75G
EST1-
RR-KF
25G
100G
50G
75G
EST1-
RR-QKR
25G
100G
50G
75G

Supp. Fig 3

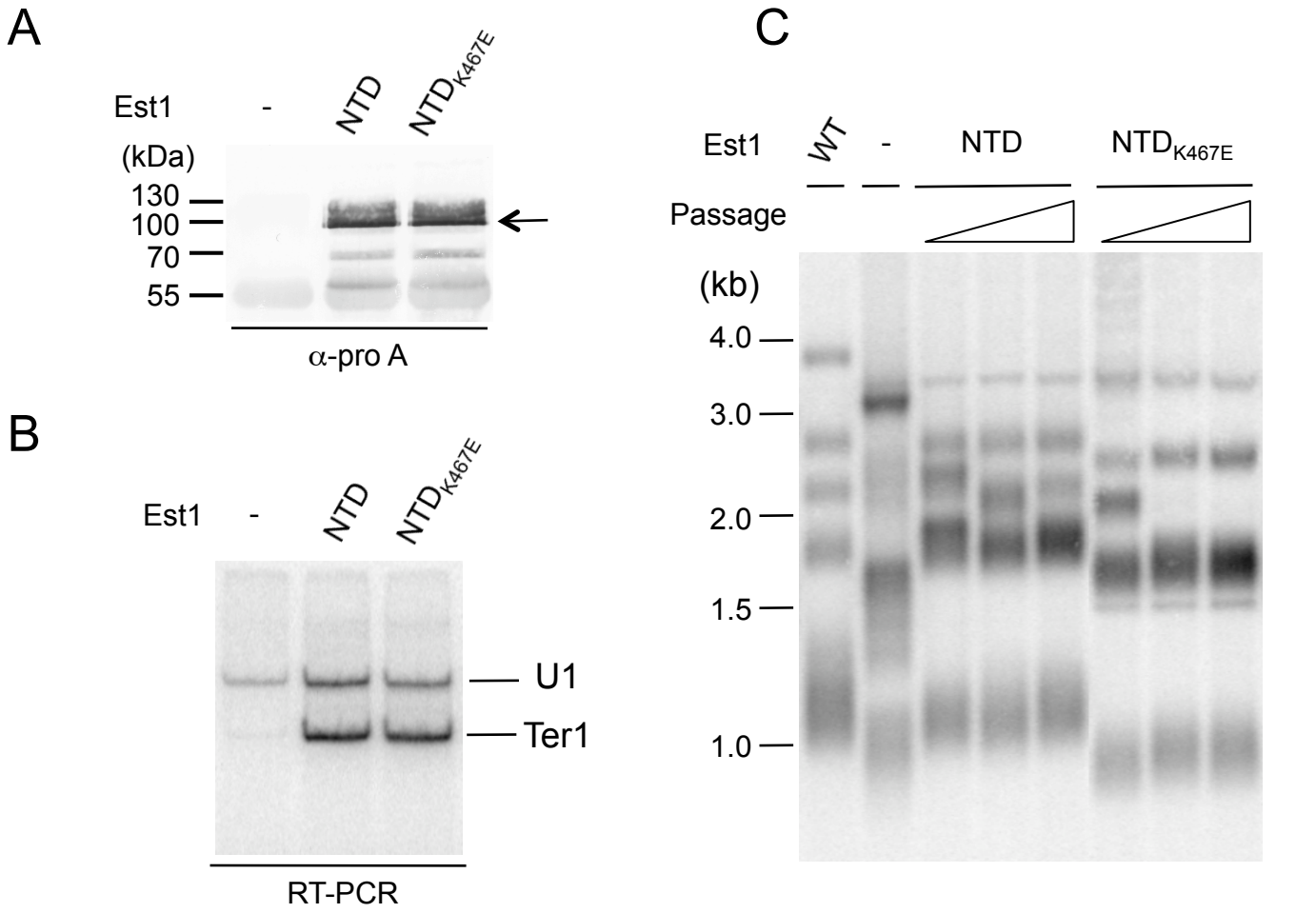
A
Est1
-
NTD
NTDK467E
(kDa)
130
100
70
55
α-pro A
B
Est1
-
NTD
NTDK467E
U1
Ter1
RT-PCR
C
Est1
WT
-
NTD
NTDK467E
Passage
(kb)
4.0
3.0
2.0
1.5
1.0

Supp. Fig. 4

A

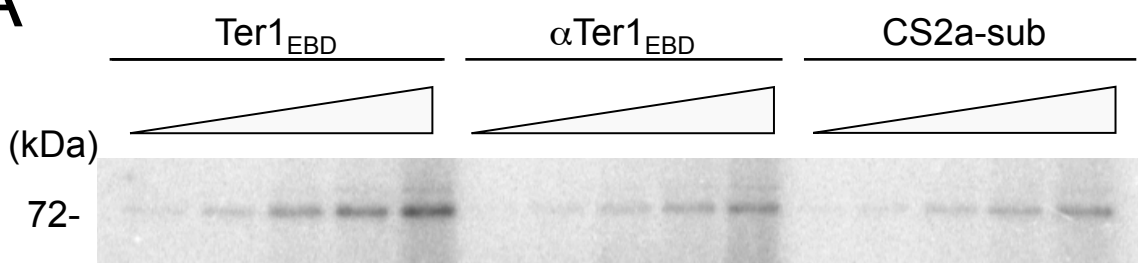
Ter1EBD
αTer1EBD
CS2a-sub
(kDa)
72-

B

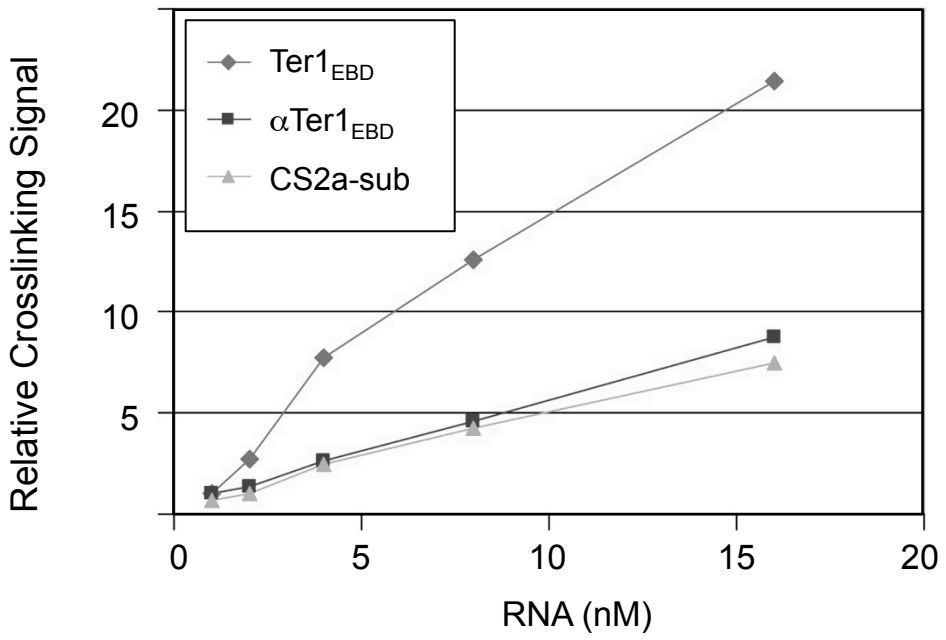
Ter1EBD
αTer1EBD
CS2a-sub
Relative Crosslinking Signal
0
5
10
15
20
RNA (nM)

Supp. Fig. 5

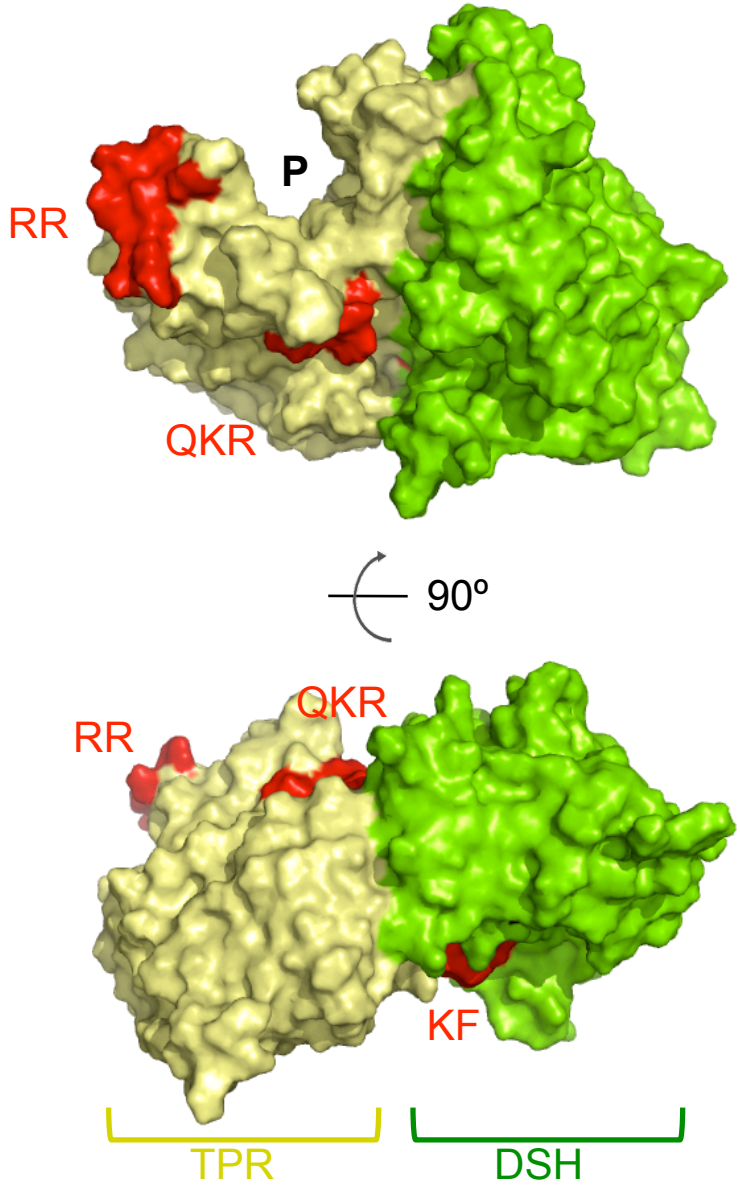

Supp. Fig. 6